

# RSC Advances



This is an *Accepted Manuscript*, which has been through the Royal Society of Chemistry peer review process and has been accepted for publication.

*Accepted Manuscripts* are published online shortly after acceptance, before technical editing, formatting and proof reading. Using this free service, authors can make their results available to the community, in citable form, before we publish the edited article. This *Accepted Manuscript* will be replaced by the edited, formatted and paginated article as soon as this is available.

You can find more information about *Accepted Manuscripts* in the [Information for Authors](#).

Please note that technical editing may introduce minor changes to the text and/or graphics, which may alter content. The journal's standard [Terms & Conditions](#) and the [Ethical guidelines](#) still apply. In no event shall the Royal Society of Chemistry be held responsible for any errors or omissions in this *Accepted Manuscript* or any consequences arising from the use of any information it contains.



## Red-emitting phosphors $\text{Na}_2\text{XF}_6: \text{Mn}^{4+}$ (X = Si, Ge, Ti) with high colour-purity for warm white-light-emitting diodes

Zhengliang Wang,\* Yong Liu, Yayun Zhou, Qiang Zhou,\* Huiying Tan, Qiuhan Zhang and Jinhui Peng

Received 00th January 2015,  
Accepted 00th January 2015

DOI: 10.1039/x0xx00000x

www.rsc.org/

Red-emitting phosphors  $\text{Na}_2\text{XF}_6: \text{Mn}^{4+}$  (X = Si, Ge, Ti) are synthesized by a simple co-precipitation method. The crystal structure, morphology and composition of as-prepared phosphors are characterized by X-ray diffraction (XRD), scanning electron microscopy (SEM), energy-dispersive X-ray spectrometer (EDS) and atomic absorption spectroscopy (AAS). Their optical properties were investigated by photo-luminescent spectra (PL), diffuse reflectance spectra (DRS), and the luminescence decay curves. These phosphors exhibit broad excitation band in blue regions and intense emission in red regions with high color-purity. The sample  $\text{Na}_2\text{SiF}_6: \text{Mn}^{4+}$  shares bright red emission under blue light excitation, and its CIE coordinates are  $x = 0.684$ ,  $y = 0.315$ , which are close to the NTSC (National Television Standard Committee) standard values for red ( $x = 0.67$ ,  $y = 0.33$ ). The white-light-emitting diodes (WLEDs) fabricated with this phosphor emits intense warm white-light with lower color temperature (3930 K) and higher color rendering index (92.3). The above results indicated that red phosphor  $\text{Na}_2\text{SiF}_6: \text{Mn}^{4+}$  maybe serve as a red-emitting phosphor for application in warm WLEDs.

### Introduction

White-light-emitting diodes (WLEDs) have received gradually increasing interest, owing to their high efficiency, long lifetime, energy-saving and environmental friendly properties.<sup>1–3</sup> So far, the commercial WLEDs were mainly fabricated by the combination of yellow phosphor  $\text{Y}_3\text{Al}_5\text{O}_{12}: \text{Ce}^{3+}$  (YAG) with blue GaN-LED chips ( $\lambda_{\text{em}} \approx 460$  nm), which have low colour rendering index ( $R_a$ ) and high colour temperature ( $T_c$ ) because of the absence of red components in their spectra.<sup>4–6</sup> To obtain warm white-light, some red phosphors were mixed with YAG phosphor on GaN chips to neutralize the cold white light.<sup>7,8</sup> In general, a suitable red-emitting phosphor for blue LED chip should meet the following necessary conditions: 1) the phosphor is of high stability; 2) the production-cost is low; 3) the phosphor exhibits strong absorption around 460 nm and strong red-emitting with the appropriate chromaticity coordinates near the NTSC (National Television Standard Committee) standard values. At present, rare-earth ions  $\text{Eu}^{2+}$  or  $\text{Ce}^{3+}$  activated (oxy)nitride compounds red phosphors have been developed and applied in WLEDs system.<sup>9–11</sup> However, these (oxy)nitride phosphors still have several drawbacks: 1) a large part of the red emission is beyond 650 nm, which decreases the luminous efficiency (LE) of radiation; 2) the preparation needs extremely harsh conditions such as high temperature and reducing atmosphere, which increase their

production-cost.<sup>12</sup> Hence it is urgent to exploit new red phosphors with high colour-purity and low production-cost for warm WLEDs.

In recent years, much interest was paid on  $\text{Mn}^{4+}$ -activated alkaline/alkaline earth hexafluoride phosphors (such as  $\text{K}_2\text{XF}_6: \text{Mn}^{4+}$  and  $\text{BaXF}_6: \text{Mn}^{4+}$ , X = Si, Ti and Ge), since their excellently narrow emission under blue light excitation.  $\text{K}_2\text{XF}_6: \text{Mn}^{4+}$  and  $\text{BaXF}_6: \text{Mn}^{4+}$  have been prepared by many methods, including co-precipitation method, hydrothermal method and wet chemical etching method.<sup>13–21</sup> For example, in our previous work,<sup>20</sup> we hydrothermally synthesized  $\text{BaGeF}_6: \text{Mn}^{4+}$  red phosphor and investigated its potential application in WLED devices. Compared with  $\text{K}_2\text{XF}_6: \text{Mn}^{4+}$  and  $\text{BaXF}_6: \text{Mn}^{4+}$ ,  $\text{Na}_2\text{XF}_6: \text{Mn}^{4+}$  (X = Si, Ti and Ge; denoted as NXFM) exhibit intense red emission with higher colour-purity, due to higher zero phonon line (ZPL) emission.<sup>22–26</sup> Adachi prepared  $\text{Na}_2\text{SiF}_6: \text{Mn}^{4+}$  and  $\text{Na}_2\text{GeF}_6: \text{Mn}^{4+}$  by wet chemical etching of Si wafers or Ge shots in  $\text{HF}/\text{NaMnO}_4$  mixed solution, and investigated their photo-luminescent properties.<sup>22,23</sup> However, this method to prepare these phosphors has some drawbacks, such as expensive cost of raw materials (Si wafers or Ge shots) and low yield. Recently, Liu demonstrated the co-precipitation approach to synthesize  $\text{Na}_2\text{SiF}_6: \text{Mn}^{4+}$  from a silicon fluoride solution using  $\text{H}_2\text{O}_2$  to reduce  $\text{Mn}^{7+}$  to  $\text{Mn}^{4+}$  at room temperature.<sup>26</sup> This approach to synthesize  $\text{Na}_2\text{SiF}_6: \text{Mn}^{4+}$  is very feasible. However the growth of  $\text{Na}_2\text{SiF}_6: \text{Mn}^{4+}$  is hard to control, because the redox reaction between  $\text{H}_2\text{O}_2$  and  $\text{NaMnO}_4$  in HF solution is very fast.

In this article, red phosphors NXFM were synthesized by co-precipitation method without any reductants. Compared with other methods to prepared  $\text{Mn}^{4+}$ -activated hexafluoride phosphors, this co-precipitation method is very simple and feasible. All the obtained products exhibit intensive red light

Key Laboratory of Comprehensive Utilization of Mineral Resources in Ethnic Regions, Joint Research Centre for International Cross-border Ethnic Regions Biomass Clean Utilization in Yunnan, School of Chemistry and Biotechnology, Yunnan Minzu University, Kunming, 650500, P. R. China.

\* Prof. Zhengliang Wang, Email: wangzhengliang@foxmail.com.

Electronic Supplementary Information (ESI) available: [details of diffuse reflectance spectra and decay curves]. See DOI: 10.1039/x0xx00000x

with high colour-purity under blue light excitation, which maybe find application in warm WLEDs.

## Experimental

### Synthesis

All the raw materials including  $\text{SiO}_2$ ,  $\text{TiO}_2$ ,  $\text{GeO}_2$ ,  $\text{NaF}$ ,  $\text{HF}$ , and  $\text{NaMnO}_4 \cdot \text{H}_2\text{O}$  are of analytical grade without further purification. Commercial YAG was purchased from Shenzhen Quanjing Photon Co. Ltd., China. The synthesis process of NXFM is shown in Fig. 1. In a typical synthesis, 2.5 mmol  $\text{XO}_2$  ( $\text{X} = \text{Si, Ge, Ti}$ ) was adequately dissolved in 5 ml 40%  $\text{HF}$  solution. Then 0.5 mmol  $\text{NaMnO}_4 \cdot \text{H}_2\text{O}$  was added into the transparent solution. When the solution was heated to  $70^\circ\text{C}$ , 5 mmol  $\text{NaF}$  was slowly added into the solution, which was kept at  $70^\circ\text{C}$  for 30 min under continuous stirring. At last the precipitates were washed with methanol for several times and dried at  $80^\circ\text{C}$  for 2 hours.

The single red LEDs were fabricated by combining GaN chips with as-prepared phosphors. Firstly, the mixtures of NXFM and epoxy resin (mass ratio is 1:1) were coated on GaN chips and solidified. Then the devices were packaged with epoxy resin and solidified at  $150^\circ\text{C}$  for 1 h. At last the red LEDs were obtained. The WLEDs were fabricated *via* the similar method with the mixtures of commercial YAG, NXFM and epoxy resin (mass ratio is 1:0.5:16).



**Fig. 1** Schematic diagram of the preparation process for NXFM phosphors *via* chemical co-precipitation method.

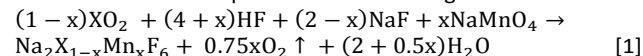
### Characterizations

The crystal structure was initially characterized using powder X-ray diffraction (XRD) with a X-ray diffractometer using  $\text{Cu K}\alpha$  radiation ( $\lambda = 0.15406 \text{ nm}$ ) and a graphite monochromator operating at 40 kV and 30 mA from  $15^\circ$  to  $70^\circ$  with a scanning step of  $0.02^\circ$  at  $4^\circ \text{ min}^{-1}$ . The as-prepared products for morphology and composition were observed by scanning electron microscopy (SEM, FEI Quanta 200 Thermal FE Environment scanning electron microscopy) with an attached energy-dispersive X-ray spectrometer (EDS). The doping amount of  $\text{Mn}^{4+}$  in the as-prepared samples was measured on a Shimadzu AA-6300 atomic absorption spectrophotometer (AAS) with  $\text{HNO}_3$  (68%) as solvent and acetylene flame as heat source. Thermogravimetry (TG) and differential scanning calorimeter (DSC) curves were measured on a Netzsch STA449 C thermal analyzer at a heating rate  $10^\circ\text{C}/\text{min}$  under  $\text{N}_2$ . The diffuse reflectance spectra (DRS) were collected on a Cary 5000 UV-Vis-NIR spectrophotometer, and the luminescence decay curves were obtained from an FLS920 fluorescence spectrophotometer. Photo-luminescence (PL) spectra were

documented on a Cary Eclipse FL1011M003 (Varian) spectrofluorometer, and the xenon lamp was used as excitation source. The performance of LEDs was recorded on a high accurate array spectrometer (HSP6000)

## Results and discussion,

In current work, NXFM phosphors were prepared *via* the co-precipitation method, and  $\text{MnF}_6^{2-}$  was obtained by the decomposition of  $\text{Na}_2\text{MnO}_4$  in  $\text{HF}$  solution without  $\text{H}_2\text{O}_2$ . The chemical reaction is represented as following:



The phases of as-prepared NXFM were investigated by XRD, and the representative results are shown in Fig. 2. The XRD patterns of  $\text{Na}_2\text{SiF}_6 \cdot \text{Mn}^{4+}$  and  $\text{Na}_2\text{GeF}_6 \cdot \text{Mn}^{4+}$  are consistent with the corresponding JCPDS cards of  $\text{Na}_2\text{SiF}_6$  (No. 33-1280) and  $\text{Na}_2\text{GeF}_6$  (No. 35-0814), no impurity can be found. This result indicates that the obtained phosphors  $\text{Na}_2\text{SiF}_6 \cdot \text{Mn}^{4+}$  and  $\text{Na}_2\text{GeF}_6 \cdot \text{Mn}^{4+}$  are of single phase with the similar hexagonal structure (space group of  $P321$ ). In this hexagonal structure,  $\text{Si}^{4+}/\text{Ge}^{4+}$  occupies the center of  $\text{SiF}_6^{2-}/\text{GeF}_6^{2-}$  octahedron.  $\text{Na}_2\text{TiF}_6 \cdot \text{Mn}^{4+}$  also has single phase according its XRD pattern compared with the JCPDS card of  $\text{Na}_2\text{TiF}_6$  (No. 15-0581). In current work,  $\text{Na}_2\text{TiF}_6 \cdot \text{Mn}^{4+}$  has the hexagonal structure with space group of  $P-3m1$ , this crystal structure is different from the trigonal structure of  $\text{Na}_2\text{TiF}_6 \cdot \text{Mn}^{4+}$  reported by Adachi.<sup>24</sup> In this structure of  $\text{Na}_2\text{TiF}_6$ ,  $\text{Ti}^{4+}$  was also coordinated by six  $\text{F}^-$  to form a  $\text{TiF}_6^{2-}$  octahedron. Since  $\text{Mn}^{4+}$  has the same charge as  $\text{Si}^{4+}$ ,  $\text{Ge}^{4+}$  and  $\text{Ti}^{4+}$ , and its radius (53 pm,  $\text{CN} = 6$ ) is close to that of  $\text{Si}^{4+}$  (40 pm,  $\text{CN} = 6$ ),  $\text{Ge}^{4+}$  (53 pm,  $\text{CN} = 6$ ) and  $\text{Ti}^{4+}$  (61 pm,  $\text{CN} = 6$ ), the doping of  $\text{Mn}^{4+}$  does not change the structure of hosts  $\text{Na}_2\text{XF}_6$ , then  $\text{Mn}^{4+}$  maybe occupy the sites of  $\text{XF}_6^{2-}$  ( $\text{X} = \text{Si, Ge, Ti}$ ) octahedron.

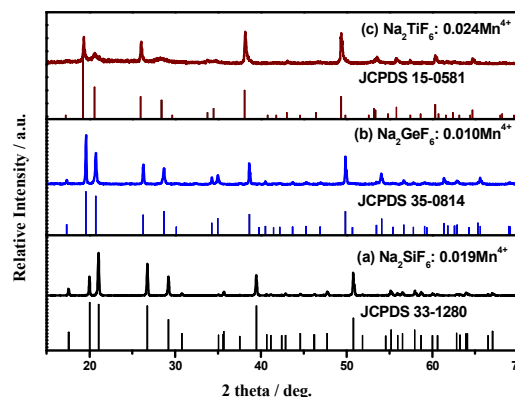


**Fig. 2** XRD patterns of (a)  $\text{Na}_2\text{SiF}_6 \cdot 0.019\text{Mn}^{4+}$ , (b)  $\text{Na}_2\text{GeF}_6 \cdot 0.010\text{Mn}^{4+}$  and (c)  $\text{Na}_2\text{TiF}_6 \cdot 0.024\text{Mn}^{4+}$ .

The morphology and composition of the obtained NXFM products were examined by SEM and EDS analysis, and the representative results are shown in Fig. 3. Obviously, the obtained products exhibit an irregular morphology with smooth surfaces. Closely inspecting the particle size distribution among them, it can be found that the  $\text{Na}_2\text{SiF}_6 \cdot \text{Mn}^{4+}$  product displayed an apparent larger size ( $\sim 20 \mu\text{m}$ ) than that of  $\text{Na}_2\text{GeF}_6 \cdot \text{Mn}^{4+}$  ( $\sim 0.8 \mu\text{m}$ ) and  $\text{Na}_2\text{TiF}_6 \cdot \text{Mn}^{4+}$  ( $\sim 0.5 \mu\text{m}$ ) products. Three curves in Fig. 3 are their corresponding EDS

results. It can be clearly observed the peaks belonging to F, Si, K, and Mn elements from Fig. 3(a2), which indicates that Mn element has been indeed doped into the matrix lattice to occupy the lattice site of Si, and the doping amount of  $Mn^{4+}$  in  $Na_2SiF_6: Mn^{4+}$  product is 1.9 mol %, measured from AAS analysis. Similar results can be obtained from  $Na_2TiF_6: Mn^{4+}$  and  $Na_2GeF_6: Mn^{4+}$  products in Fig. 3(b2-c2), whose doping amount of  $Mn^{4+}$  are 2.4 mol % and 1.0 mol %, respectively. Moreover, the absence of oxygen peak in the these EDS spectra implies that there is no  $MnO_2$  produced during this precipitation process.

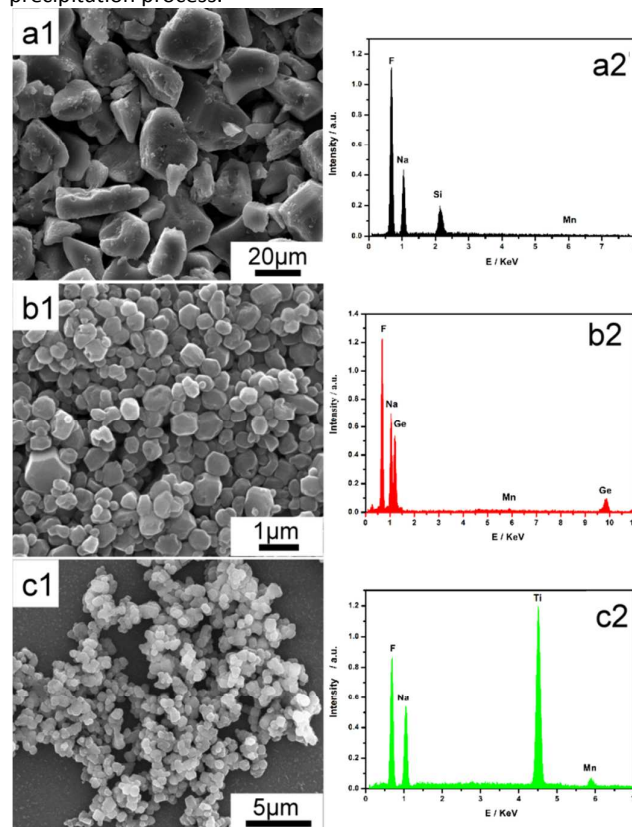


**Fig. 3** SEM images and EDS spectra of (a<sub>1</sub>, a<sub>2</sub>)  $Na_2SiF_6: Mn^{4+}$ , (b<sub>1</sub>, b<sub>2</sub>)  $Na_2GeF_6: Mn^{4+}$  and (c<sub>1</sub>, c<sub>2</sub>)  $Na_2TiF_6: Mn^{4+}$ .

### Optical properties

Fig. 4 is the excitation and emission spectra of NXFM. These phosphors exhibits the similar excitation spectra with two broad bands located at  $\sim 350$  nm and  $\sim 465$  nm, which can be assigned to the  ${}^4A_{2g} \rightarrow {}^4T_{2g}$  transitions and  ${}^4A_{2g} \rightarrow {}^4T_{1g}$  transitions of  $Mn^{4+}$ , respectively. The red emissions of these phosphors between 600 and 650 nm are due to the spin-forbidden  ${}^2E_g \rightarrow {}^4A_{2g}$  transition of  $Mn^{4+}$ . And the strongest emission peak is located at  $\sim 627$  nm, which has some blue shift compared with that of  $K_2TiF_6: Mn^{4+}$  ( $\sim 632$  nm).<sup>12</sup> The emission peaks located at  $\sim 609$ , 617, 627, 631, 642 nm are ascribed as the transitions of the  $\nu_6(t_{2u})$ , zero phonon line (ZPL),  $\nu_6(t_{2u})$ ,  $\nu_4(t_{1u})$ ,  $\nu_3(t_{1u})$  vibronic modes, respectively.<sup>27</sup> Intense ZPL emission of these phosphors can be found in these emission spectra, this result is different from that of  $K_2XF_6: Mn^{4+}$  and  $BXF_6: Mn^{4+}$ .<sup>18-21</sup> Compared with  $Na_2GeF_6: Mn^{4+}$  and  $Na_2TiF_6: Mn^{4+}$ ,  $Na_2SiF_6: Mn^{4+}$  exhibits the strongest red emission under 465 nm excitation. The CIE coordinates

according to the emission spectra of  $Na_2SiF_6: Mn^{4+}$ ,  $Na_2GeF_6: Mn^{4+}$  and  $Na_2TiF_6: Mn^{4+}$  are calculated to be ( $x = 0.684$ ,  $y = 0.315$ ), ( $x = 0.685$ ,  $y = 0.315$ ) and ( $x = 0.683$ ,  $y = 0.316$ ), which are very close to the NTSC standard values for red ( $x = 0.67$ ,  $y = 0.33$ ).

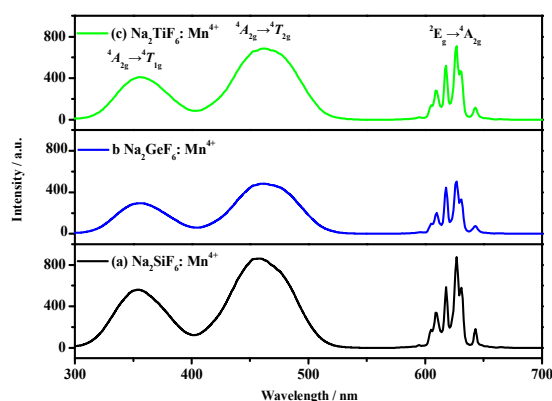


**Fig. 4** The excitation ( $\lambda_{em} = 627$  nm) and emission ( $\lambda_{ex} = 465$  nm) spectra of (a)  $Na_2SiF_6: Mn^{4+}$ , (b)  $Na_2GeF_6: Mn^{4+}$  and (c)  $Na_2TiF_6: Mn^{4+}$ .

Fig. S1 is the diffuse reflectance spectra of  $Na_2SiF_6$  and  $Na_2SiF_6: Mn^{4+}$ . Comparing with  $Na_2SiF_6$ ,  $Na_2SiF_6: Mn^{4+}$  exhibits two obvious absorption bands at  $\sim 350$  nm and  $\sim 465$  nm in curve b, which are due to the absorption of  $Mn^{4+}$  in  $Na_2SiF_6: Mn^{4+}$ , this result is in agreement with the excitation spectrum of  $Na_2SiF_6: Mn^{4+}$ . Fig. S2 shows the decay curves for  ${}^2E_g \rightarrow {}^4A_2$  (627 nm) of the  $Mn^{4+}$  in  $Na_2SiF_6: Mn^{4+}$ ,  $Na_2GeF_6: Mn^{4+}$  and  $Na_2TiF_6: Mn^{4+}$  red phosphors. These curves are fitted into single-exponential function, and their lifetime  $\tau$  values are 3.74 ms, 3.68 ms and 2.68 ms, respectively.

### Fabrication and Performance of LED Devices

Since LEDs usually work at a temperature below  $150$  °C,<sup>27</sup> the thermal stability is an important parameter for phosphors. As shown in Figure 5, TG and DSC curves of  $Na_2SiF_6: Mn^{4+}$  show that its thermal decomposition temperature ( $T_d$ ) is about  $400$  °C. Such high decomposition temperature suggests that this phosphor has high thermal stability and it is enough to be applied in WLED devices.

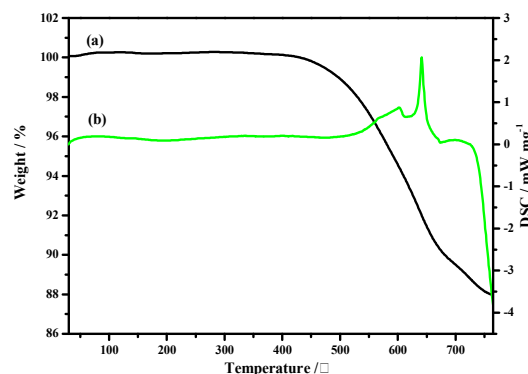


**Fig. 5** (a) TG and (b) DSC curves of  $Na_2SiF_6: Mn^{4+}$ .

To investigate the potential applications of these red phosphors, the single red LEDs and WLEDs were fabricated by combining blue GaN chips, the red phosphors NXFM with or without commercial YAG. Fig. 6 is the electro-luminescent (EL) spectra of the single red LEDs based on NXFM phosphors under 20 mA current excitation. The emission of LED chip is at  $\sim 465$  nm, and its half-peak width is about 20 nm. Compared with curve a, the emission of LED chip cannot be observed in curve b, indicating that  $\text{Na}_2\text{SiF}_6: \text{Mn}^{4+}$  can efficiently absorb the emission of LED chip. The red emission between 600 and 650 nm is due to the emission of  $\text{Na}_2\text{SiF}_6: \text{Mn}^{4+}$ . Bright red light can be observed from this red LED based on  $\text{Na}_2\text{SiF}_6: \text{Mn}^{4+}$ . The red LEDs based on  $\text{Na}_2\text{GeF}_6: \text{Mn}^{4+}$  and  $\text{Na}_2\text{TlF}_6: \text{Mn}^{4+}$  share similar EL spectra. Different from curve b, the emission of LED chip still exist in the EL spectra of red LEDs based on  $\text{Na}_2\text{GeF}_6: \text{Mn}^{4+}$  and  $\text{Na}_2\text{TlF}_6: \text{Mn}^{4+}$ . This result showed that the absorption efficiency of  $\text{Na}_2\text{GeF}_6: \text{Mn}^{4+}$  and  $\text{Na}_2\text{TlF}_6: \text{Mn}^{4+}$  is lower than that of  $\text{Na}_2\text{SiF}_6: \text{Mn}^{4+}$ , which is in agreement with their excitation spectra.

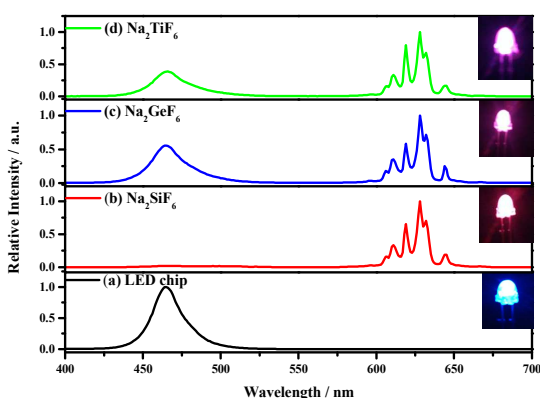


**Fig. 6** EL spectra of (a) the GaN-LED chip, the red LEDs based on (b)  $\text{Na}_2\text{SiF}_6: \text{Mn}^{4+}$ , (c)  $\text{Na}_2\text{GeF}_6: \text{Mn}^{4+}$  and (d)  $\text{Na}_2\text{TlF}_6: \text{Mn}^{4+}$  under 20 mA current excitation, the inserted figures are the images of the red LEDs.

Fig. 7 is the EL spectra of WLEDs with or without NXFM. Curve a is the EL spectrum of WLED without NXFM. The white light was obtained by combining the blue emission of LED chip and yellow emission of YAG. Since the emission of YAG in red regions is very weak, this WLED shows high  $T_c$  (8440 K) and low  $R_a$  (78.4). With the introduction of NXFM, red emission peaks can be observed obviously at 609 nm, 617 nm, 627 nm, 631 nm and 642 nm, which are due to the  ${}^2E_g \rightarrow {}^4A_2$  of  $\text{Mn}^{4+}$  in NXFM. And the emission of LED chip get weaker. Among the four curves, the red emission intensity of  $\text{Na}_2\text{SiF}_6: \text{Mn}^{4+}$  is the strongest. Bright white light can be observed by naked eyes from these WLEDs, when they were excited with 20 mA current. The relative performance of the WLEDs is summarized in Table 1. The warm WLED based on  $\text{Na}_2\text{SiF}_6: \text{Mn}^{4+}$  shows excellent optical performance:  $T_c = 3930$  K,  $R_a = 92.3$ ,  $LE = 69.21$  lm/W. These results demonstrated that this red phosphor has potential applications in warm LEDs.

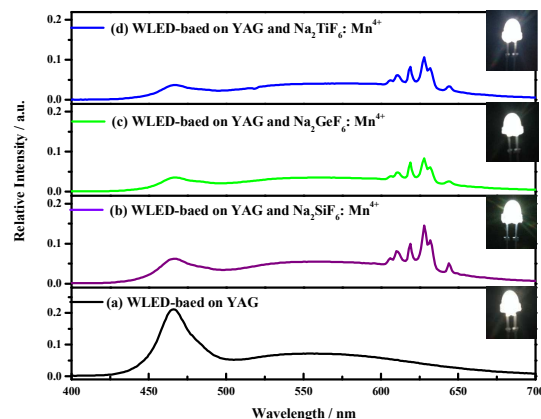


**Fig. 7** EL spectra of the WLEDs based on (a) YAG, (b)  $\text{Na}_2\text{SiF}_6: \text{Mn}^{4+}$  and YAG, (c)  $\text{Na}_2\text{GeF}_6: \text{Mn}^{4+}$  and YAG, (d)  $\text{Na}_2\text{TlF}_6: \text{Mn}^{4+}$  and YAG under 20 mA current excitation, the inserted figures are the images of the WLEDs.

**Table 1** Performance of the WLEDs coated with: (a) YAG, (b) YAG and  $\text{Na}_2\text{SiF}_6: \text{Mn}^{4+}$ , (c) YAG and  $\text{Na}_2\text{GeF}_6: \text{Mn}^{4+}$ , (d) YAG and  $\text{Na}_2\text{TlF}_6: \text{Mn}^{4+}$  at 20 mA forward current.

WLEDs	$T_c$ (K)	$R_a$	LE (lm/W)	CIE (x, y)
a	8440	78.4	78.31	(0.286, 0.314)
b	3930	92.3	63.21	(0.389, 0.397)
c	3554	92.1	46.71	(0.410, 0.412)
d	3841	90.7	34.21	(0.396, 0.409)

## Conclusions

$\text{Na}_2\text{XF}_6: \text{Mn}^{4+}$  red phosphors were prepared by the co-precipitation method, and their structure, morphology and luminescent properties were investigated. Among all the as-prepared NXFM samples, red phosphor  $\text{Na}_2\text{SiF}_6: \text{Mn}^{4+}$  shows the strongest absorption band in blue-light region and the strongest red emission with appropriate CIE coordinates ( $x = 0.684$ ,  $y = 0.315$ ). The WLED based on  $\text{Na}_2\text{SiF}_6: \text{Mn}^{4+}$  and commercial YAG exhibits intense white-light emission with lower  $T_c$  and higher  $R_a$ . These results suggest that  $\text{Na}_2\text{SiF}_6: \text{Mn}^{4+}$  phosphor is a promising red phosphor for WLEDs.

## Acknowledgements

This work was supported by National Nature Science Foundation of China (No. 21261027), the Natural Science Foundation of Yunnan Province, and Department of Yunnan Education (Grants 2014FB147 and 2014Y253), and Program for Innovative Research Team (in Science and Technology) in University of Yunnan Province (2011UY09) and Yunnan Provincial Innovation Team (2011HC008).

## Notes and references

- 1 S. Nakamura, *Solid State Commun.*, 1997, **102**, 237
- 2 E. F. Schubert and J. K. Kim, *Science*, 2005, **308**, 1274.
- 3 S. Pimputkar, J. S. Speck, S. P. DenBaars and S. Nakamura, *Nat. Photonics*, 2009, **3**, 180.
- 4 C. C. Lin and R. S. Liu, *J. Phys. Chem. Lett.*, 2011, **2**, 1268.
- 5 H. S. Jang; W. B. Im, D. C. Lee, D. Y. Jeon and S. S. Kim, *J. Lumin.*, 2007, **126**, 371.
- 6 X. J. Wang, G. H. Zhou, H. L. Zhang, H. L. Li, Z. J. Zhang and Z. Sun, *J. Alloys Compd.*, 2012, **519**, 149.
- 7 K. A. Denault, A. A. Mikhailovsky, S. Brinkley, S. P. DenBaars and R. Seshadri, *J. Mater. Chem. C*, 2013, **1**, 1461.
- 8 R. J. Xie and N. Hirotsuki, *Sci. Technol. Adv. Mat.*, 2007, **8**, 588.
- 9 C. J. Duan, X. J. Wang, W. M. Otten, A. C. A. Delsing, J. T. Zhao, and H. T. Hintzen, *Chem. Mater.*, 2008, **20**, 1597.
- 10 W. B. Park, S. P. Singh, C. Yoon and K. S. Sohn, *J. Mater. Chem.*, 2012, **22**, 14068.
- 11 S. Yamada, H. Emoto,; M. Ibukiyama and N. Hirotsuki, *J. Eur. Ceram. Soc.*, 2012, **32**, 1355.
- 12 H. M. Zhu, C. C. Lin, W. Q. Luo, S. T. Shu, Z. G. Liu, Y. S. Liu, J. T. Kong, E. Ma, Y. G. Cao, R. S. Liu and X. Y. Chen, *Nat. Commun.*, 2014, **5**, 4312.
- 13 X. Q. Li, X. M. Su, P. Liu, J. Liu, Z. L. Yao, J. J. Chen, H. Yao, X. B. Yu and M. Zhan, *CrystEngComm.*, 2015, **17**, 930.
- 14 J. H. Oh, H. Kang, Y. J. Eo, H. K. Park and Y. R. Do, *J. Mater. Chem. C*, 2015, **3**, 607.
- 15 L. L. Wei, C. C. Lin, M. H. Fang, M. G. Brik, S. F. Hu, H. Jiao and R. S. Liu, *J. Mater. Chem. C*, 2015, **3**, 1655.
- 16 L. F. Lv, Z. Chen, G. K. Liu, S. M. Huang and Y. X. Pan, *J. Mater. Chem. C*, 2015, **3**, 1935.
- 17 C. X. Liao, R. P. Cao, Z. J. Ma, Y. Li, G. P. Dong, K. N. Sharafudeen and J. R. Qiu, *J. Am. Ceram. Soc.*, 2013, **96**, 3552.
- 18 R. Kasa and S. Adachi, *J. Electrochem. Soc.*, 2012, **159**, J89.
- 19 T. Takahashi and S. Adachi, *J. Electrochem. Soc.*, 2008, **155**, E183.
- 20 Q. Zhou, Y. Y. Zhou, Y. Liu, L. J. Luo, Z. L. Wang, J. H. Peng, J. Yan and M. M. Wu, *J. Mater. Chem. C*, 2015, **3**, 3055.
- 21 X. Y. Jiang, Y. X. Pan, S. M. Huang, X. A. Chen, J. G. Wang and G. K. Liu, *J. Mater. Chem. C*, 2014, **2**, 2301.
- 22 Y. K. Xu and Adachi, *S. J. Appl. Phys.*, 2009, **105**, 013525.
- 23 T. Arai and S. Adachi, *J. Appl. Phys.*, 2011, **110**, 063514.
- 24 Y. K. Xu and S. Adachi, *J. Electrochem. Soc.*, 2011, **158**, J58.
- 25 S. Adachi, H. Abe and R. Kasa, T. Arai, *J. Electrochem. Soc.*, 2012, **159**, J34.
- 26 H. D. Nguyen, C. C. Lin, M. H. Fang and R. S. Liu, *J. Mater. Chem. C*, 2014, **2**, 10268.
- 27 H. Wang, P. He, S. Liu, J. Shi, M. Gong, *Appl. Phys. B*, 2009, **97**, 481.